Structural Changes during the Photocycle of Photoactive Yellow Protein Monitored by Ultraviolet Resonance Raman Spectra of Tyrosine and Tryptophan

Samir F. El-Mashtoly,[†] Seigo Yamauchi,[†] Masato Kumauchi,[‡] Norio Hamada,[§] Fumio Tokunaga,[‡] and Masashi Unno*[,†]

Institute of Multidisciplinary Research for Advanced Materials, Tohoku University, Sendai 980-8577, Japan, Department of Earth and Space Science, Graduate School of Science, Osaka University, Toyonaka, Osaka 560-0043, Japan, and JST, CREST, Osaka University, Suita, Osaka 565-0871, Japan

Received: August 24, 2005; In Final Form: October 19, 2005

Photoactive yellow protein (PYP) is a bacterial blue light photoreceptor, and photoexcitation of dark-state PYP (PYP_{dark}) triggers a photocycle that involves several intermediate states. We report the ultraviolet resonance Raman spectra of PYP with 225−250 nm excitations and investigate protein structural changes accompanying the formation of the putative signaling state denoted PYP_M. The PYP_M−PYP_{dark} difference spectra show several features of tyrosine and tryptophan, indicating environmental changes for these amino acid residues. The tyrosine difference signals show small upshifts with intensity changes in Y8a and Y9a bands. Although there are five tyrosine residues in PYP, Tyr42 and Tyr118 are suggested to be responsible for the difference signals on the basis of a global fitting analysis of the difference spectra at different excitation wavelengths and the crystal structure of PYP_{dark}. A further experiment on the Thr50→Val mutant supports environmental changes in Tyr42. The observed upshift of the Y8a band suggests a weaker or broken hydrogen bond between Tyr42 and the chromophore in PYP_M. In addition, a reorientation of the OH group in Tyr42 is suggested from the upshift of the Y9a band. For tryptophan, the Raman bands of W3, W16, and W18 modes diminish in intensity upon formation of PYP_M. The loss of intensities is attributable to an exposure of tryptophan in PYP_M. PYP contains only one tryptophan (Trp119) that is located more than 10 Å from the active site. Thus the observed changes are indicative of global conformational changes in protein during the transition from PYP_{dark} to PYP_M. These results are in line with the currently proposed photocycle mechanism of PYP.

The photoactive yellow protein (PYP) offers a convenient system for the study of conformational motions in proteins. This protein gains further attention as the structural prototype for the PAS (Per-ARNT-Sim) and LOV (light, oxygen, or voltage) domains of a large class of receptor proteins.[1] PYP is the 125-residue, 14-kDa cytosolic photoreceptor proposed to mediate negative phototaxis[2] in the phototrophic bacterium *Halorhodospira halophila*. This protein has an α/β fold, consisting of a central β-sheet with the 4-hydroxycinnamyl chromophore and an N-terminal cap (Figure 1). In a dark state (PYP_{dark}), the phenolate anion of the *trans*-chromophore[3−5] is stabilized by hydrogen bonds with Tyr42 and Glu46.[6,7] The side chain oxygen of Thr50 hydrogen bonds with the OH group of Tyr42. Lowering the pH induces the formation of a bleached state denoted $PYP_{M,dark}$, which contains a protonated *trans*-chromophore[7] and a partially disordered protein moiety.[8−10] Photoexcitation of PYP_{dark} triggers a photocycle that involves, at least, three intermediate states denoted PYP_L (also called I_1 or pR), $PYP_{M'}$ (also called pB′), and PYP_M (also called I_2 or pB).[11−13] The photoisomerization of the chromophore produces the deprotonated *cis*-chromophore in PYP_L. The transition from PYP_L to $PYP_{M'}$ involves protonation of the phenolic oxygen of the chromophore, whereas large structural changes of the protein take place during the $PYP_{M'}$ to PYP_M transition.[5,13−16] A long-lived PYP_M intermediate is the putative signaling state of this photoreceptor protein.

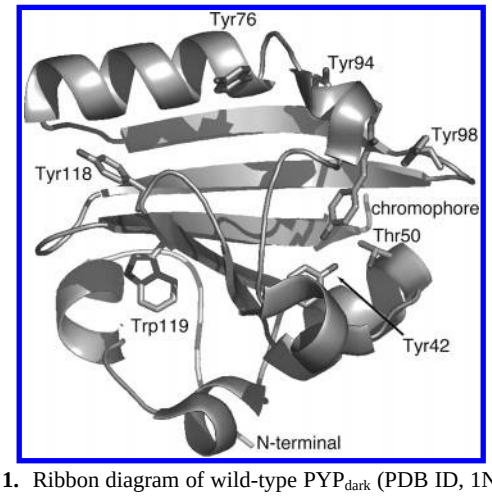

Figure 1. Ribbon diagram of wild-type PYP_{dark} (PDB ID, 1NWZ; ref 3). The 4-hydroxycinnamyl chromophore and tryptophan, tyrosine, and Thr50 residues are shown. The N-terminal is also designated in the figure.

Because of a possible functional significance, extensive studies have been made to analyze the structure of PYP_M. Time-resolved X-ray crystallography revealed that the structural alterations upon transition from PYP_{dark} to PYP_M are limited to the vicinity of the chromophore.[17] However, spectroscopic studies have shown larger structural alterations for PYP_M in solution.[9,13,18−29] For example, an NMR study indicated that

* To whom correspondence should be addressed. Telephone: +81-22-217-5618. Fax: +81-22-217-5616. E-mail: unno@tagen.tohoku.ac.jp.
[†] Tohoku University.
[‡] Graduate School of Science, Osaka University.
[§] JST.

10.1021/jp054772z CCC: $30.25
Published on Web 11/19/2005

PYP_M is disordered to a significant degree with multiple conformations that exchange on a millisecond time scale.[18] In fact, time-resolved Fourier transform infrared (FTIR) studies of PYP under both crystalline and solution conditions have demonstrated that the structure of PYP_M differs in the two phases.[13] Thus it is crucial to characterize the structure of PYP_M in aqueous solution.

One of the important issues concerning the structure of PYP_M is related to structural changes of the chromophore and in nearby amino acid residues such as Tyr42 and Glu46 (Figure 1). The structural changes in the active site during the photocycle have been studied with a wide range of techniques. For instance, resonance Raman spectroscopy has revealed the chromophore structure,[4,5,15,16,30−33] whereas the protonation state of Glu46 has been determined by FTIR studies.[13,21,34] However, structural and environmental changes in Tyr42 during the photocycle of PYP in solution are uncovered, because few spectroscopic methods other than ultraviolet resonance Raman (UVRR) spectroscopy mentioned below directly investigate tyrosine residues in proteins. Another important issue is related to the structural changes in the protein moiety. Several studies pointed out a significant conformational change in the N-terminal cap upon illumination.[20,22,24,26−28] For instance, a small-angle X-ray scattering experiment of PYP suggested that the structural change in the N-terminus reduces the globularity in PYP_M.[22]

To characterize further the structure of PYP_M in aqueous solution, we have applied UVRR spectroscopy to wild-type (WT) PYP and some mutants (Glu→Gln; E46Q, Thr→Val; T50V) for the first time. Raman spectroscopy can provide structural information via the sensitivity of vibrational bands to molecular conformation and environmental changes.[35,36] If the excitation wavelength is out of resonance with the electronic transitions of a sample, both the chromophore and protein moieties contribute to Raman spectra.[35,37] However, excitation at wavelengths below 250 nm results in strong enhancement of vibrational modes for aromatic residues such as tyrosine and tryptophan, with little or no interference from the chromophore. The selective enhancement of aromatic residues in UVRR spectroscopy has proved useful for a variety of chromoproteins such as retinal proteins.[35,36] Thus UVRR spectra of PYP directly probe structural and/or environmental changes in Tyr42. Furthermore, UVRR spectroscopy will yield information on the N-terminal cap through tryptophan Raman bands, because PYP contains one tryptophan residue at position 119, which is sandwiched between the central β-sheet and the N-terminus.[3] As discussed below, the UVRR data provide new information on the protein structural changes during the formation of PYP_M.

Materials and Methods

Sample Preparation. Production of WT PYP and E46Q and T50V mutant apoproteins from *Escherichia coli*, reconstitution of the holoprotein with the chromophore, and the subsequent protein purification were performed as described previously with minor modifications.[38,39] For most of the measurements of PYP_{dark} and PYP_M, PYP was dissolved in 10 mM Tris·HCl buffer at pH 7.4 with 0.2 M sodium perchlorate ($NaClO_4$) as a Raman internal intensity standard. PYP in buffered D_2O (90% D_2O/10% H_2O) was prepared by proper dilution of a concentrated protein in 100 mM Tris·HCl buffer at pH 7.4 into D_2O, and then the sample was incubated overnight at room temperature before the measurements.

Resonance Raman Spectroscopy. The UVRR spectrometer is composed of a Nd:YAG laser pumped optical parametric oscillator (OPO) laser (Spectra-Physics Inc., MOPO730), a 0.5 m single spectrometer (Spex 500M) equipped with a 3600 groove/mm holographic grating, and a liquid nitrogen cooled CCD detector (Instrument S.A., Inc.) (Figure 2). A Nd:YAG laser (Spectra-Physics Inc., Pro270) was run at 20 Hz and produced a 355 nm pulse to pump an OPO laser. The 450−500 nm light from the OPO laser was frequency doubled with a BBO crystal (Spectra-Physics Inc., FDO-900) to generate 225−250 nm light of ca. 5 ns pulse width. The OPO laser is wavelength tunable with a simple mechanism and is applicable to measure UVRR spectra at different excitation wavelengths. This system is operated to produce 3 μJ/pulse at the sample. A 90° scattering geometry was employed, and the scattered photons were collected and focused onto the entrance slit of a spectrometer by using two quartz plano convex lenses. A polarization scrambler was placed at the entrance slit to remove the effects of polarization from the spectrometer throughput. A Triax190 spectrometer (Instrument S.A., Inc.) removed the excitation light, and the first order of the dispersed light by the 500M spectrometer was imaged on the detector. An entrance slit width of 0.2 mm corresponds to a spectral resolution of 14 cm^{-1} for the 240 nm excitation. All spectra were taken at room temperature (~23 °C), and homemade software eliminated the noise spikes in the spectra caused by cosmic rays. All Raman spectra were calibrated by using neat cyclohexane as a standard, and we have an approximately 2 cm^{-1} accuracy in this calibration. Relative frequency shifts, however, can be determined with much greater accuracy, ca. ±0.2 cm^{-1}. Sample volumes were 100 μL and were contained in a quartz spinning cell (10 mm in diameter). The cell was spun at 800 rpm.

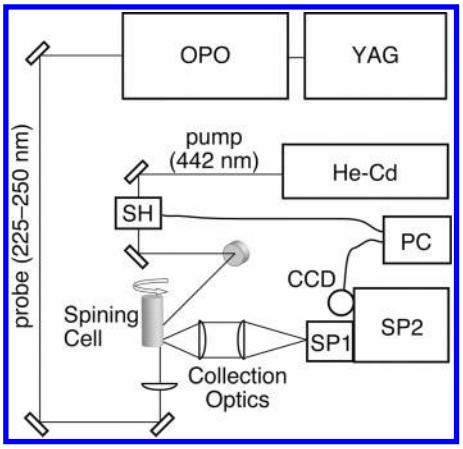

Figure 2. Raman spectrometer consisting of a Nd:YAG laser (YAG) pumped optical parametric oscillator laser (OPO), a spinning cell, and a 0.5 m single spectrometer (SP2) with a 0.19 m spectrometer (SP1) and a CCD detector. The pump light is obtained by a He−Cd laser (He−Cd). Illumination of the pump light was controlled by a shutter (SH), which is regulated by a personal computer (PC).

For the measurements of PYP_M, the sample solutions were irradiated by 441.6 nm light from a helium−cadmium laser (Kimmon Electric Co., Ltd., IK5651R-G) to produce the intermediate state as a photostationary state. The pump beam was spatially displaced from the probe beam to avoid a fluorescence generated by the pump beam as well as possible contamination of short-lived intermediates such as PYP_L (see Figure 2). The experimental conditions for the pump beam were optimized from an independent resonance Raman experiment with 325.0 nm excitation, which probes the chromophore vibrational modes for PYP_M.[5,15,16] The necessary pump power was determined by increasing the pump power until the intensity of the ν_{13}/ν_{14} doublet[16] of the chromophore no longer changed. This criterion was met at 22 mW. Acquisition of PYP_{dark} and PYP_M spectra was carried out in an alternating way: the Raman

signals of PYP_{dark} were collected for 60 s, followed by a 60 s collection of PYP_M signals. This cycle was repeated more than 60 times to improve the signal-to-noise ratio of the spectra. This procedure minimized the effect of fluctuations of the laser power during the measurements and allowed us to use the same samples for the measurement of PYP_{dark} and PYP_M. The spectral intensities were normalized by adjusting the heights of the perchlorate bands at 934 cm^{-1} to be the same in the PYP_{dark} and PYP_M spectra. The normalized spectra of PYP_{dark} were subtracted from that of PYP_M to give difference spectra. Note that PYP precipitated at pH 2 in the presence of high concentration of salts. Thus we performed the experiments with low pH samples without an internal standard. The effect of sample degradation during the measurements was corrected as described previously.[16]

Global Fitting Analysis. Gaussian function is used as the spectral band shape for a fitting analysis. Here we express the Raman intensity at ν_i cm^{-1} as $G(\nu_i,I,\nu,\Delta\nu_w)$, where I, ν, and $\Delta\nu_w$ are peak intensity, peak frequency, and bandwidth, respectively. First we consider an ideal situation that the number of a particular type of chromophoric group such as tyrosine in a protein is m, and each of those gives the same Raman intensity I_0 and frequency ν. If the Raman bands for n out of m chromophoric groups change their intensity and/or frequency, the difference spectrum $\Delta I(\nu_i)$ before and after the change is as follows:

$$\Delta I(\nu_i) = G(\nu_i,nI_1,\nu+\Delta\nu,\Delta\nu_w) - G(\nu_i,nI_0,\nu,\Delta\nu_w) \quad (1)$$

where I_1 is a Raman intensity after the change, and $\Delta\nu$ is a frequency shift. In a real situation, each chromophoric group has a different environment with different I_0, I_1, ν, and $\Delta\nu_w$. Hence eq 1 approximately describes the difference spectrum, and the parameters I_0, I_1, ν, $\Delta\nu$, and $\Delta\nu_w$ can be considered as average values. For a global fitting analysis, n, ν, $\Delta\nu$, and $\Delta\nu_w$ are the same for all i, and I_0 is determined by an observed Raman intensity divided by m.

Raman Excitation Profile. The Raman excitation profile is a plot of Raman band intensities versus excitation wavelengths. Intensities were determined from the measured peak height ratio I_N/I_S for the bands of the sample (N) and internal standard (S) using

$$\sigma_N = \sigma_S(I_N/I_S)[(\nu_0-\nu_S)/(\nu_0-\nu_N)]^4(C_S/C_N) \quad (2)$$

where σ_N and σ_S are the absolute Raman cross sections of the band being determined and of the internal standard band, respectively, C_S/C_N is the concentration ratio, ν_0 is the laser excitation frequency, and ν_N and ν_0 are the vibrational frequencies of the sample and standard Raman bands, respectively. In this study, we mainly utilized sodium perchlorate as an internal standard. The σ_S value for the 934 cm^{-1} mode of perchlorate was previously determined.[40]

Results

UVRR Spectra of WT PYP_{dark}. The upper two traces in Figure 3 are the UVRR spectra of WT PYP_{dark} at 240 (trace a) and 230 (trace b) nm excitations. These spectra contain several Raman bands that mainly arise from tyrosine and tryptophan residues, and their mode labels (Y for tyrosine, W for tryptophan)[35] are indicated in the figure. Raman bands of tyrosine are observed at 1614 (Y8a, ring C−C stretching), 1207 (Y7a, ring−C stretching), and 1174 cm^{-1} (Y9a, CH in-plane bending). We also observed the tyrosine Fermi doublet at 832/852 cm^{-1}, which is due to resonance between the symmetric ring-breathing

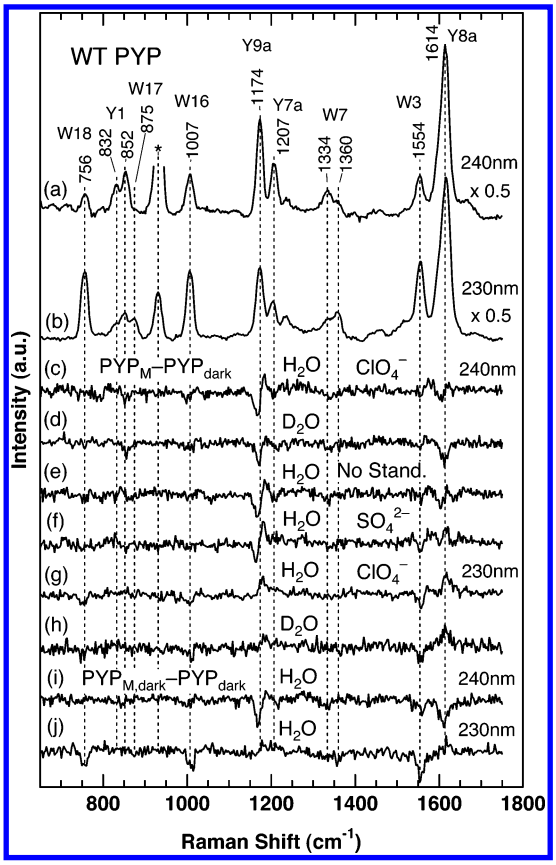

Figure 3. UVRR spectra of wild-type PYP_{dark} with (a) 240 and (b) 230 nm excitations and PYP_M minus PYP_{dark} (c−h) and $PYP_{M,dark}$ minus PYP_{dark} (i,j) difference spectra. The protein concentration was 150 μM in all experiments. The following list gives buffer composition and excitation wavelength: (a, c) 10 mM Tris·HCl, pH 7.4, 0.2 M $NaClO_4$, λ_{ex} = 240 nm; (b, g) 10 mM Tris·HCl, pH 7.4, 0.2 M $NaClO_4$, λ_{ex} = 230 nm; (d) 90% D_2O/10% H_2O with 10 mM Tris·HCl, pD 7.4, λ_{ex} = 240 nm; (e) 10 mM Tris·HCl, pH 7.4, λ_{ex} = 240 nm; (f) 10 mM Tris·HCl, pH 7.4, 0.2 M Na_2SO_4, λ_{ex} = 240 nm; (h) 90% D_2O/10% H_2O with 10 mM Tris·HCl, pD 7.4, λ_{ex} = 230 nm; and (i, j) 10 mM Tris·HCl, pH 7.4 for PYP_{dark} and 10 mM citrate/20 mM phosphate, pH 2.0 for $PYP_{M,dark}$, (i) λ_{ex} = 240 nm, (j) λ_{ex} = 230 nm. The asterisk indicates a Raman band of ClO_4^-.

Y1 and the overtone 2Y16a of the nonplanar ring vibration at ~413 cm^{-1}.[41] In addition to tyrosine, we observed several Raman bands for a tryptophan residue. The bands at 1554, 1007, and 756 cm^{-1} are assigned to W3 (C−C stretching of the pyrrole ring), W16 (benzene ring-breathing), and W18 (indole ring-breathing), respectively. A doublet at 1360/1334 cm^{-1} is ascribed to W7. This doublet arises from a Fermi resonance between a fundamental mode at ~1340 cm^{-1} and a combination of two out-of-plane modes involving the benzene and pyrrole rings comprising the tryptophan side chain.[35] Figure 3 also illustrates the marked changes in the UVRR spectra of PYP_{dark} at 240 and 230 nm excitations. For instance, a new band appears at 875 cm^{-1} with 230 nm excitation. This band is assigned to W17, which arises from a mixture of a benzene ν_{12}-like ring-breathing mode with some motion of the NH group.[35] The differences in the spectra are due to the fact that tyrosine and tryptophan have electronic transitions at different wavelengths.[35] For example, the tyrosine Raman bands of Y8a, Y7a, and Y9a are in resonance with the L_a transition, which is observed at 223 nm with ϵ = 8400 M^{-1} cm^{-1} in aqueous solution.[35,36,42] On the other hand, the tryptophan bands of W3, W16, and W18 are enhanced in resonance with the B_b transition, which has

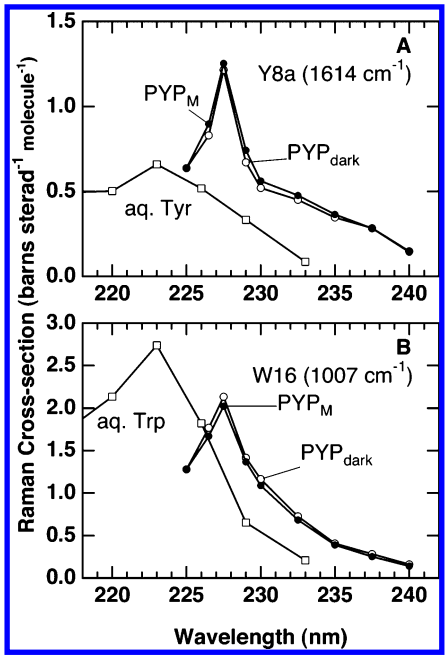

Figure 4. Raman excitation profiles for (A) Y8a and (B) W16 bands of wild-type PYP_{dark} (○) and wild-type PYP_M (●). The band intensities are given in units of cross section using the 934 cm^{-1} ClO_4^- band as an internal reference. The data for aqueous tyrosine and tryptophan (□) were taken from ref 43.

been assigned to the 218 nm absorption with $\epsilon = 34\,000$ M^{-1} cm^{-1} in aqueous solution.[35,36]

The dependence of Raman intensity on excitation wavelength (Raman excitation profile, REP) reveals clearly protein effects on electronic transitions of chromophoric groups such as tyrosine and tryptophan.[36] Figure 4 presents the REPs of tyrosine (Y8a) and tryptophan (W16) in PYP_{dark} and in aqueous amino acids.[43] The REPs for tyrosine and tryptophan in PYP_{dark} are red-shifted (~900 cm^{-1}) as a result of the protein environment, which lowers the energy of the resonant electronic transitions. Similar red shifts of the REP for tyrosine and tryptophan are observed in other proteins such as hemoglobin.[43] Note that, in some cases, the REP maximum is slightly shifted from the relevant electronic transition;[35,36,42] e.g., the REP of W16 for aqueous tryptophan maximizes near 223 nm, which is 5 nm longer than the B_b absorption maximum of 218 nm.[43]

Difference of the UVRR Spectra between PYP_M and PYP_{dark}. The lower part of Figure 3 (traces c−h) demonstrates the PYP_M−PYP_{dark} difference spectra under different experimental conditions. In this study, PYP_M was produced as a photostationary state. As the photocycle intermediates preceding PYP_M such as PYP_L and $PYP_{M'}$ have shorter lifetimes than PYP_M by a factor of more than 100-fold (the lifetimes of PYP_L, $PYP_{M'}$, and PYP_M are ca. 250 μs, 2 ms, and 350 ms, respectively),[12,13,21] their populations are negligible under the present conditions.[44] Trace c is the difference spectrum at 240 nm excitation in the presence of 0.2 M ClO_4^- as an internal intensity standard. The 934 cm^{-1} ClO_4^- band was used to normalize the spectra for subtraction as described in the Experimental Section. Trace e is the difference spectrum in the absence of the internal standard, and the spectrum of PYP_{dark} was subtracted from that of PYP_M without normalization. As can be seen, traces c and e are similar, indicating that the presence of 0.2 M ClO_4^- little affects the UVRR spectra of PYP. Trace f is the difference spectrum in the presence of 0.2 M SO_4^{2-}. In contrast to the case of ClO_4^-, the difference spectrum with SO_4^{2-} (trace f) is different from the one without an internal standard (trace e) or from the one with ClO_4^- (trace c). This indicates that the presence of SO_4^{2-} perturbs the PYP_M−PYP_{dark} difference spectrum, and we use ClO_4^- in the following studies. In many cases, an internal standard is essential for UVRR spectroscopy, even though the pump−probe and probe-only spectra are obtained under identical conditions, because the absorption spectrum may vary for the intermediate states, leading to nonconstant self-absorption. In the present case, however, the normalization factors were usually close to unity, indicating that the self-absorption is not significantly changed between PYP_{dark} and PYP_M.

As described above, Figure 3 demonstrates that some of the tryptophan and tyrosine Raman bands give rise to difference features, which reflect intensity changes and/or frequency shifts. With 240 nm excitation (trace c), most of the notable features in the difference spectrum arise from tyrosine residues. The negative features near 1605 and 1207 cm^{-1} imply that both Y8a and Y7a show a lower intensity for PYP_M than for PYP_{dark}. A characteristic sigmoidal difference feature at ~1175 cm^{-1} indicates an upshift of the Y9a mode in PYP_M. For tryptophan, a small feature for W7 can be discerned around 1360−1330 cm^{-1} in traces c−f, although the observed change is not clear under the signal-to-noise ratio of the observed spectra. As expected for the altered resonance conditions, the overall pattern of the difference spectra changes drastically as excitation wavelength varies from 240 to 230 nm (from trace c to trace g). With 230 nm excitation (trace g), the W3, W16, and W18 bands of tryptophan show negative features in the difference spectrum, indicating a lower intensity for PYP_M than for PYP_{dark}. The other significant differences between the two excitations are features for Y8a, Y7a, and Y9a. Trace c shows a negative band at ~1605 cm^{-1} for Y8a. This feature disappears in trace g, but a positive feature appears at ~1615 cm^{-1}. In the Y9a region, the sigmoidal difference feature at ~1175 cm^{-1} becomes a positive band, when the excitation wavelength changes from 240 to 230 nm. We have also measured the UVRR spectra of PYP_M at different excitation wavelengths, and Figure 4 compares REPs of Y8a and W16 between PYP_M and PYP_{dark}.

Here we should consider the possibility that the difference feature around 1610 cm^{-1} may be due to Y8b, because the frequencies of the Y8a and Y8b modes are similar.[35] Normal-coordinate calculations have shown that Y8a and Y8b are predominantly C−C stretching vibrations of the phenolic ring with little involvement of the OH group for Y8a.[45] On deuteration of the phenolic OH group, Y8b downshifts ca. 6 cm^{-1}, whereas Y8a does not shift significantly. To distinguish between Y8a and Y8b, we examined the effect of D_2O on the difference spectra of PYP_M minus PYP_{dark}. Traces d and h in Figure 3 are the difference spectra of PYP in D_2O at 240 and 230 nm excitations, respectively. As can be seen, deuterium substitution of exchangeable protons such as a hydroxyl hydrogen of tyrosine (traces c,d and g,h) does not downshift the difference signals around 1610 cm^{-1}, excluding a possibility that the observed features are due to Y8b.

We also comment on the possibility that the chromophore contributes to the UVRR spectra of PYP. This is actually the case for the UVRR experiments with 250 nm excitation. As shown in Figure 1S (Supporting Information), the PYP_M−PYP_{dark} difference spectrum with 250 nm excitation shows new features around 1280 and 1585 cm^{-1}. Because isotopic substitution of the chromophore clearly affects the difference spectrum (traces f and g in Figure 1S), the features observed with 250 nm excitation are attributable to the Raman bands of the chromophore. A comparison of the difference spectra with the

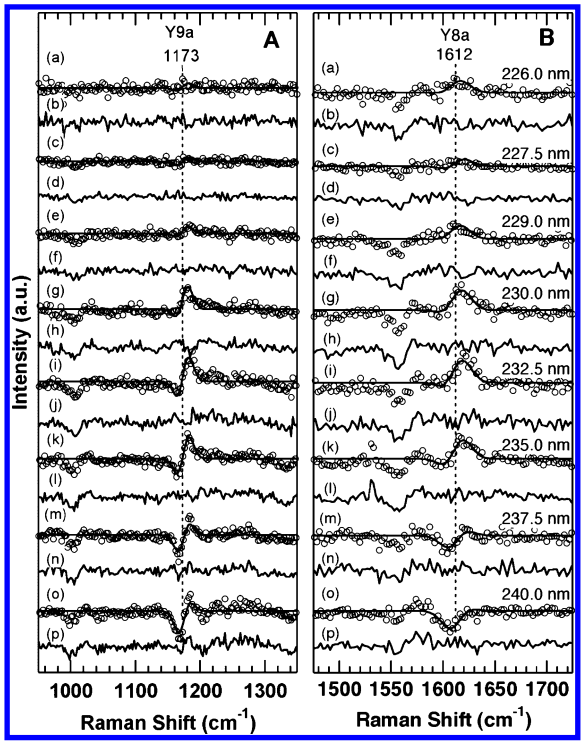

Figure 5. PYP_M minus PYP_{dark} difference UVRR spectra of (A) Y9a and (B) Y8a regions for indicated eight different excitation wavelengths between 226 and 240 nm. Open circles in traces a, c, e, g, i, k, m, and o represent the experimental data, while the solid lines are fit with the global fitting analysis. The residuals from the fit are shown as traces b, d, f, h, j, l, n, and p. The global fitting analysis for Y9a and Y8a was performed in the 1050−1280 and 1570−1700 cm^{-1} regions, respectively.

resonance Raman spectra of PYP_M with 325 nm excitation (traces h and i in Figure 1S) indicates that the features at ∼1280 and ∼1585 cm^{-1} can be assigned to ν_{22}/ν_{23} and ν_{13}/ν_{14} of the protonated *cis*-chromophore, respectively.[15,16] Because these features are not observed below 240 nm, the UVRR data with 225−240 nm excitations are discussed in this study.

Previous studies suggested that PYP_M has structural similarities to the acid-induced denatured state $PYP_{M,dark}$.[8−10] Thus we measured the UVRR spectra of $PYP_{M,dark}$ at pH 2.0 and compared those with PYP_M. Traces i and j in Figure 3 are the difference spectra between $PYP_{M,dark}$ and PYP_{dark} at 240 and 230 nm excitation, respectively. As can be clearly seen in the difference spectra, the formation of $PYP_{M,dark}$ affects the UVRR spectra of PYP, especially in the following three points: (i) The Y8a band at ∼1615 cm^{-1} is diminished in intensity with 240 nm excitation, whereas this band gains intensity with 230 nm excitation. (ii) The difference spectra exhibit sigmoidal difference features around 1175 cm^{-1}, implying an upshift of the Y9a band. (iii) The difference spectrum with 240 nm excitation shows a negative band for W3. Negative features are also detected for W3, W16, and W18 with 240 nm excitation, indicating diminished intensities for these Raman bands in $PYP_{M,dark}$. Although these difference spectra are not simple copies of those between PYP_M and PYP_{dark}, the observed changes associated with the formation of $PYP_{M,dark}$ are also characteristic of PYP_M.

Global Fitting Analysis of Tyrosine Bands in the PYP_M−PYP_{dark} Difference Spectra. Parts A and B, respectively, of Figure 5 show the difference spectra between PYP_M and PYP_{dark} in the Y9a and Y8a regions. Although the difference spectra around Y9a show a positive feature near 1180 cm^{-1} with 230 nm excitation, a sigmoidal difference feature becomes pronounced above 232.5 nm excitation. Analogously, the positive feature observed at ∼1615 cm^{-1} with shorter wavelength excitation is replaced by a sigmoidal or a negative feature above 235 nm excitation. To analyze these data, we have performed a global fitting analysis using eq 1. Because PYP contains five tyrosine residues, the peak intensities I_0 in eq 1 were set to one-fifth of the total intensities of the Y9a or Y8a band. The solid lines in Figure 5 are the fitting results, and the corresponding parameters are summarized in Table 1. As can be seen in the figure, the global fitting procedure provides a reasonable fit to the data for both Y9a and Y8a regions. This implies that the features observed in the PYP_M−PYP_{drak} difference spectra are due to frequency shifts as well as intensity changes of the Y9a and Y8a Raman bands. In addition, the number of tyrosine residues (n) that contribute to the difference spectra is estimated to be two, which suggests that two tyrosine residues show average upshifts ($\Delta\nu$) of 2.7 and 0.7 cm^{-1} for Y9a and Y8a, respectively. Here we should stress that the results from the global fitting analysis are not conclusive. For instance, it is possible that Raman bands of more than two tyrosine residues shift in different directions. In this case, the observed shift comes from cancellation of real shifts, and the global fitting analysis provides only a clue to a minimum shift associated with the formation of PYP_M.

TABLE 1: Summary of Global Fitting Analysis[a]

	ν/cm^{-1}	$\Delta\nu$/cm^{-1}	$\Delta\nu_w$/cm^{-1}	n
Y9a	1173	2.7	22	2.1
Y8a	1612	0.7	24	2.0

[a] The global fitting analysis for Y9a and Y8a was performed in the 1050−1280 and 1570−1700 cm^{-1} regions, respectively. See text for details.

UVRR Spectra of E46Q and T50V Mutants. To investigate further the structure of PYP_M, we have measured the UVRR spectra of the T50V and E46Q mutants. The X-ray structure of PYP_{dark}[3] shows that the phenolate oxygen of the chromophore hydrogen bonds with the hydroxyl group of Tyr42 and the protonated carboxylate of Glu46. The side chain of Thr50 hydrogen bonds to the hydroxyl oxygen of Tyr42. Because the hydrogen bond between Tyr42 and Thr50 is absent in the mutant T50V,[46] this mutation is anticipated to affect the Raman bands of Tyr42. Figure 6 displays the UVRR spectrum of WT PYP_{dark} with 240 nm excitation (trace a) as well as the difference spectra between T50V and WT proteins for PYP_{dark} (trace b) and PYP_M (trace c). As expected, the T50V mutation significantly affects the Raman bands of tyrosine. The difference spectrum for PYP_{dark} (trace b) displays prominent features that are due to bands for the Y8a, Y7a, and Y9a tyrosine modes. The sigmoidal difference features indicate that these Raman bands upshift when Thr50 is replaced with valine. Some of the tryptophan Raman bands also show small features in the difference spectrum; e.g., the W16 mode at 1007 cm^{-1} upshifts by ∼2 cm^{-1} in the mutant. Although the difference spectrum for PYP_M (trace c) also shows clear features for tyrosine Raman bands, an inspection of the two difference spectra reveals that the effects of the T50V mutation are different between PYP_{dark} and PYP_M. The tyrosine Y8a band of PYP_M gives rise to a weaker difference signal compared to that of PYP_{dark}, whereas the Y9a feature is stronger in PYP_M than that in PYP_{dark}. In addition, the sigmoidal difference feature of the Y7a band in PYP_{dark} is not clear in PYP_M. These results suggest that the Raman bands of Tyr42 are changed when PYP_{dark} is converted to PYP_M. This implies that Tyr42 contributes to the difference features in the difference spectra between PYP_M and PYP_{dark}. In fact, Figure 6 shows that the T50V mutation perturbs the PYP_M minus PYP_{dark}

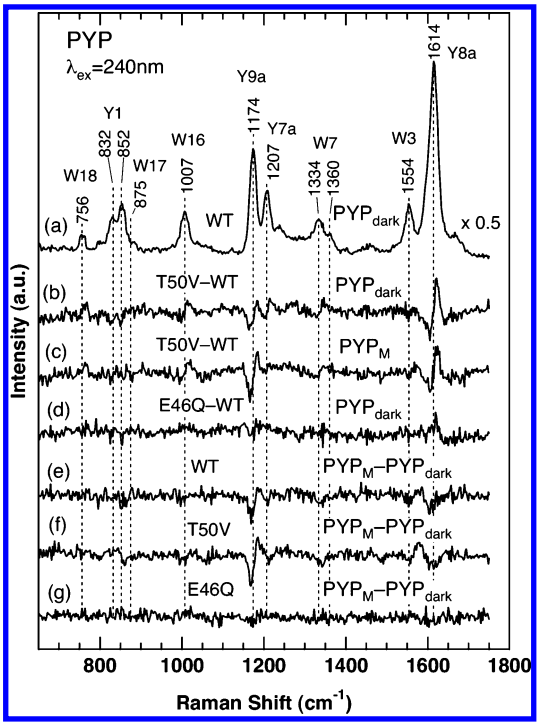

Figure 6. UVRR and difference spectra for wild-type PYP and T50V and E46Q mutants. Trace a is the UVRR spectrum of wild-type PYP_{dark}. Traces b, c, and d are the difference spectra for T50V minus wild-type PYP_{dark}, T50V minus wild-type PYP_M, and E46Q minus wild-type PYP_{dark}, respectively. Traces e, f, and g are the PYP_M minus PYP_{dark} difference spectra for wild-type PYP, T50V, and E46Q mutants, respectively. The spectra were obtained at 240 nm excitation, and all samples were dissolved in 10 mM Tris·HCl buffer at pH 7.4.

difference spectrum (traces e and f). For instance, the Y9a mode upshifts by $\sim$1 cm^{-1} upon formation of PYP_M in the case of WT PYP, whereas it upshifts by $\sim$2 cm^{-1} in the T50V mutant. Note that we did not use Tyr42 mutants such as Y42A or Y42F for the present purpose, because their spectroscopic properties are significantly changed by the mutation.[7,34,46,47]

In contrast to the T50V mutant, the E46Q mutation little affects the UVRR spectrum of PYP_{dark} (trace d). This result is reasonable because of a lack of direct interactions of Glu46 with tyrosine and tryptophan residues.[3] Furthermore, the E46Q mutant exhibits no detectable feature in the difference spectrum of PYP_M minus PYP_{dark}. Although it is possible that the fraction of PYP_M is smaller in the E46Q mutant than that in WT PYP, the results for the E46Q mutant suggest that protein structural changes associated with the formation of PYP_M are reduced by the mutation. This result is consistent with previous works that indicated that the large conformational changes observed in the WT protein are largely absent in the E46Q mutant.[13,48]

Discussion

Environment of a Tryptophan Residue in PYP_{dark}. Because of a single tryptophan residue in PYP, the observed Raman bands reflect the local environment of Trp119 (Figure 1). The frequency of the W17 band is suggested to be sensitive to the strength of hydrogen bonding at the indole nitrogen of tryptophan residue.[49] As shown in Figure 3, this band is present in PYP_{dark} at 875 cm^{-1}, a frequency that correlates with moderate hydrogen bonding of the indole nitrogen. The crystal structure of PYP_{dark}[3] shows that a water molecule, water-1020, locates within a hydrogen bonding distance (2.9 Å) with the indole nitrogen of Trp119. Thus, the UVRR data suggest that the water molecule is also present near the tryptophan residue in solution. The indole ring vibration W3 changes in frequency as a function of the torsional angle $\chi^{2,1}$ of the $C_{\delta_1}-C_\gamma-C_\beta-C_\alpha$ linkage.[50] When $|\chi^{2,1}|$ increases from 60° to 120°, the W3 frequency increases in the range of 1542−1557 cm^{-1}. The W3 frequency in PYP_{dark} is at 1554 cm^{-1} and correlates with a $|\chi^{2,1}|$ angle of 102°. This value agrees well with X-ray diffraction data, which show that Trp119 in PYP_{dark} has a $\chi^{2,1}$ value of 104.9°.[3] The bandwidth of W3, which serves as an indicator of distribution in the torsion angle, is slightly narrower (full width at half-maximum is 20.5 ± 0.5 cm^{-1}) than that of tryptophan in solution (22.7 ± 0.3 cm^{-1}) (not shown), indicating that the orientation of the indole ring is restricted within the protein environment. Figure 4B shows that the REP for W16 is red-shifted ($\sim$900 cm^{-1}) in PYP_{dark} compared with tryptophan in aqueous buffer, indicating that the environment surrounding Trp119 differs significantly from aqueous solution. This is in line with the crystal structure of PYP_{dark},[3] where Trp119 is situated at the interface between the central PAS domain and the N-terminal cap.

Environments of Tyr42 Are Changed upon Formation of PYP_M. As shown in Figures 3 and 5, the PYP_M-PYP_{dark} difference spectra exhibit clear features for the tyrosine Raman bands such as Y8a and Y9a; i.e., these modes upshift during the transition from PYP_{dark} to PYP_M. This indicates that tyrosine residues experience environmental changes between PYP_{dark} and PYP_M. In contrast to tryptophan, assignment to a specific residue is not straightforward, since there are five tyrosine residues in PYP, any of which could, in principle, contribute. However, likely sources are Tyr42 and Tyr118, because these are interior residues, whereas the other three residues, i.e., Tyr76, Tyr94, and Tyr98, are at the surface of the protein molecule (Figure 1).[3] In fact, the former two residues are expected to contribute to the difference spectra, because Tyr42 is located in the active site and Tyr118 is the immediate neighborhood of Trp119, whose environmental changes upon formation of PYP_M are discussed below. The contribution of the two residues is collaborated by the global fitting analysis of the PYP_M-PYP_{dark} difference spectra at different excitation wavelengths; the light-induced spectral alterations in Y8a and Y9a are best explained by the frequency and intensity changes in two of the five tyrosine residues (Figure 5 and Table 1). Furthermore, the UVRR experiments of the T50V mutant (Figure 6), where a hydrogen bond between Tyr42 and Thr50 is removed, support the Raman bands of Tyr42 being altered upon formation of PYP_M. Thus, the present UVRR data provide evidence for the first time for the structural and environmental changes in Tyr42 during the photocycle of PYP in solution. This point should be emphasized, because numerous spectroscopic studies including the FTIR method on PYP have failed to detect spectral signatures of tyrosine residues.[13,21,34]

Although the light-induced changes in the Raman bands of Tyr42 are evident, the frequencies as well as the amount of shift associated with the formation of PYP_M are uncertain because of the presence of five tyrosine residues in PYP. However, the global fitting analysis estimates that the frequency of the Y8a mode for Tyr42 in PYP_{dark} is 1612 cm^{-1} (Figure 5 and Table 1). The frequency of Y8a is known to be an indicator of hydrogen bonding of the tyrosine residues:[51] a decreased (increased) hydrogen bond donation by a tyrosine residue accompanies an upshift (downshift) in the Y8a mode. The estimated frequency of the Y8a mode (1612 cm^{-1}) is lower than the average frequency of five tyrosine residues (1614 cm^{-1}; Figure 3), suggesting that Tyr42 forms a relatively strong hydrogen bond in PYP_{dark}. In Table 2, we estimate hydrogen

TABLE 2: Hydrogen Bonding Parameters for Tyrosine Residues[a]

	H-bond acceptor, X	OH···X (Å)	−O−H−X (deg)	−ring−OH (deg)
Tyr42	chromophore O	1.43	170	38
Tyr76	water 1040	1.87	178	8
Tyr94[b]	Cys69 (C═O)	1.65	172	3
Tyr98	none			
Tyr118	Asp116 COO^-	1.57	176	30

[a] Calculated from the single-crystal X-ray coordinates of WT PYP_{dark} (1NWZ).[3] Distances and angles were optimized by placing a hydrogen atom 1.03 Å from the Tyr-O atom with −C−O−H = 109.5° and allowing the C−OH bond to swivel and find an optimum geometry. [b] It is possible that Tyr94 forms a hydrogen bond with a side chain hydroxyl group of Ser72. However, because the hydrogen bond with Ser72 is longer than that with Cys69, a hydrogen bond between Tyr94 and Cys69 is more likely.

bond parameters for tyrosine residues in PYP_{dark} on the basis of the crystallographic coordinate[3] and standard assumptions[51] about the location of the unobserved hydrogen atoms. This analysis indicates that the distance between the hydrogen atom and the acceptor group is distinctly shorter in Tyr42 (1.43 Å) than in the others (1.57−1.87 Å). The global fitting analysis also estimates that the Y9a frequency of Tyr42 in PYP_{dark} is 1173 cm^{-1}, which is slightly lower in frequency than the average of five tyrosine residues (1174 cm^{-1}; Figure 3). In model compounds, the Y9a band was found to be sensitive to the dihedral angle of the tyrosine OH group, shifting up in frequency when the OH bond is in the plane of the ring.[52] The lower frequency Y9a mode for Tyr42 is again compatible with the crystal structure of PYP_{dark};[3] when this angle is calculated, the OH bond is found to be well out of the plane for Tyr42 (and Tyr118), for which the angle is larger than 30° (Table 2).

In addition to the frequencies in PYP_{dark}, the global fitting analysis estimates the shifts associated with the formation of PYP_M. As shown in Table 1, the Y8a mode for Tyr42 upshifts by ∼1 cm^{-1} upon conversion to PYP_M. The small upshift suggests that the conversion from PYP_{dark} to PYP_M weakens or breaks the Tyr42-to-chromophore hydrogen bond. We also approximate that the transition from PYP_{dark} to PYP_M accompanies an ∼3 cm^{-1} upshift of the Y9a mode (Table 1). Because the structure of PYP_M is partially disordered,[18] it seems reasonable that the dihedral angle for the Tyr42 OH group is smaller in PYP_M than that in PYP_{dark}. This reorientation of the OH bond may account for the ∼3 cm^{-1} upshift for the Y9a band. The weakening or absence of the Tyr42-to-chromophore hydrogen bond as well as the in-plane OH bond in PYP_M implies an arrangement of hydrogen bonding network around Tyr42. In fact, significant changes in the environment of Tyr42 were shown by the time-resolved X-ray crystal structure of PYP_M,[53] i.e., Tyr42 has no hydrogen bond in PYP_M, and a stable in-plane OH bond is expected. Thus, although the structural changes in the protein moiety differ appreciably between solution and crystalline conditions, the active site of PYP in solution might change in a manner similar to the crystalline case.

Tryptophan UVRR Signals Probe Global Conformatiomal Changes in PYP_M. Similar to the case of tyrosine, the PYP_M−PYP_{dark} difference spectra contain some features for the tryptophan Raman bands; i.e., the W3, W16, and W18 bands decrease in intensity when PYP_M is formed (Figure 3). Analogous spectral changes are observed for $PYP_{M,dark}$ (Figure 3), where the protein moiety is partially unfolded.[8−10] The intensity of the tryptophan bands in the UVRR spectra can be used to assess the hydrophobicity of the environment surrounding tryptophan residues; i.e., larger band intensities are expected under hydrophobic environments.[51,54] A hydrogen bonding interaction at the indole nitrogen also affects the intensity of tryptophan Raman bands.[51,54] As shown in Figure 3, there is no observable change in the W17 band during the transition from PYP_{dark} to PYP_M. Since the frequency of the W17 band is sensitive to the hydrogen bonding interaction,[49] the reduced intensity of the W3, W16, and W18 bands indicates a reduced hydrophobicity local to Trp119 in PYP_M. Taken together with the result for $PYP_{M,dark}$, these UVRR data suggest that Trp119 is partially exposed to solvent upon light illumination. This conclusion is consistent with a recent fluorescence study on PYP,[24] which showed that the formation of PYP_M affects the fluorescence properties of Trp119. The results from the present UVRR and the fluorescence[24] studies indicate that the protein structural changes associated with the formation of PYP_M are not limited to the active site, because Trp119 is located more than 10 Å from the chromophore (Figure 1). The global nature of the protein structural changes is consistent with previous works that suggested the structural changes of the N-terminus in PYP_M.[9,22,24,26−28] For example, an NMR study suggested that the core of the protein in PYP_M is relatively ordered, whereas a region including the N-terminal 28 residues is partially unfolded.[9]

Here we comment on the effects of formation of PYP_M on the tryptophan Fermi doublet W7 at 1360/1334 cm^{-1}. The intensity ratio of the doublet has been used as an indicator of the hydrophobicity of the environment surrounding tryptophan residues.[55] However, a recent UVRR study on a series of model compounds and immunity proteins indicates that the conventional interpretation is unreliable for the UVRR spectra.[56] For example, Rodriguez-Mendieta et al.[56] pointed out a complex dependence of the intensity ratio on the excitation wavelength and a dependence on the model compound. Although a small feature is observed for the W7 doublet in the light-induced difference spectrum of PYP with 240 nm excitation, the interpretation of the data in terms of the protein structure awaits further studies on the W7 doublet.

Conclusion

This paper is the first report of UVRR spectra of PYP with 225−250 nm excitation. The difference spectra between PYP_{dark} and PYP_M contain several features that arise from changes in tyrosine and tryptophan vibrational modes. The spectral changes associated with the formation of PYP_M involve upshifts of the Y8a and Y9a bands of the tyrosine residues. The UVRR spectra of the T50V mutant confirm that the Raman bands of Tyr42 vary during the photocycle of PYP. The observed changes in the tyrosine Raman bands suggest that the formation of PYP_M weakens or breaks the Tyr42-to-chromophore hydrogen bond. The rearrangement of the hydrogen bond may be accompanied by the reorientation of the Tyr42 OH group. In addition to tyrosine Raman bands, the UVRR bands of W3, W16, and W18 for Trp119 diminish in intensity upon formation of PYP_M. The observed spectral change is attributable to partial exposure of Trp119 to solvent. This implies that the light-driven structural changes are not limited to the active site, because this residue is situated more than 10 Å from the active site.

We have demonstrated that UVRR spectroscopy is a powerful tool to elucidate the structural changes associated with the formation of PYP_M. The method can be applied in a time-resolved mode to monitor dynamic changes in the protein moiety using the pump−probe (picoseconds to nanoseconds) and rapid flow (microseconds to milliseconds) techniques.[44] Time-resolved UVRR studies on PYP_L and $PYP_{M'}$ are our next projects.

Acknowledgment. This work was supported by grants from the Association for the Progress of New Chemistry (M.U.) and the Ministry of Education, Culture, Science, Sports, and Technology (16570131 to M.U.).

Supporting Information Available: Figure 1S showing the UVRR spectra of PYP with 230, 240, and 250 nm excitations. This material is available free of charge via the Internet at http://pubs.acs.org.

References and Notes

(1) Pellequer, J.-L.; Wager-Smith, K. A.; Kay, S. A.; Getzoff, E. D. *Proc. Natl. Acad. Sci. U.S.A.* **1998**, *95*, 5884−5890.

(2) Sprenger, W. W.; Hoff, W. D.; Armitage, J. P.; Hellingwerf, K. J. *J. Bacteriol.* **1993**, *175*, 3096−3104.

(3) Getzoff, E. D.; Gutwin, K. N.; Genick, U. K. *Nat. Struct. Biol.* **2003**, *10*, 663−668.

(4) Kim, M.; Mathies, R. A.; Hoff, W. D.; Hellingwerf, K. J. *Biochemistry* **1995**, *34*, 12669−12672.

(5) Unno, M.; Kumauchi, M.; Sasaki, J.; Tokunaga, F.; Yamauchi, S. *Biochemistry* **2002**, *41*, 5668−5674.

(6) Devanathan, S.; Brudler, R.; Hessling, B.; Woo, T. T.; Gerwert, K.; Getzoff, E. D.; Cusanovich, M. A.; Tollin, G. *Biochemistry* **1999**, *38*, 13766−13772.

(7) El-Mashtoly, S. F.; Unno, M.; Kumauchi, M.; Hamada, N.; Fujiwara, K.; Sasaki, J.; Imamoto, Y.; Kataoka, M.; Tokunaga, F.; Yamauchi, S. *Biochemistry* **2004**, *43*, 2279−2287.

(8) Hoff, W. D.; Vanstokkum, I. H. M.; Gural, J.; Hellingwerf, K. J. *Biochim. Biophys. Acta* **1997**, *1322*, 151−162.

(9) Craven, C. J.; Derix, N. M.; Hendriks, J.; Boelens, R.; Hellingwerf, K. J.; Kaptein, R. *Biochemistry* **2000**, *39*, 14392−14399.

(10) Lee, B.-C.; Croonquist, P. A.; Hoff, W. D. *J. Biol. Chem.* **2001**, *276*, 44481−44487.

(11) Meyer, T. E.; Yakali, E.; Cusanovich, M. A.; Tollin, G. *Biochemistry* **1987**, *26*, 418−423.

(12) Hoff, W. D.; Stokkum, I. H. M.; van Ramesdonk, H. J.; van Brederode, M. E.; Brouwer, A. M.; Fitch, J. C.; Meyer, T. E.; van Grondelle, R.; Hellingwerf, K. J. *Biophys. J.* **1994**, *67*, 1691−1705.

(13) Xie, A. H.; Kelemen, L.; Hendriks, J.; White, B. J.; Hellingwerf, K. J.; Hoff, W. D. *Biochemistry* **2001**, *40*, 1510−1517.

(14) Baca, M.; Borgstahl, G. E. O.; Boissinot, M.; Burke, P. M.; Williams, D. R.; Slater, K. A.; Getzoff, E. D. *Biochemistry* **1994**, *33*, 14369−14377.

(15) Unno, M.; Kumauchi, M.; Sasaki, J.; Tokunaga, F.; Yamauchi, S. *J. Am. Chem. Soc.* **2000**, *122*, 4233−4234.

(16) Unno, M.; Kumauchi, M.; Sasaki, J.; Tokunaga, F.; Yamauchi, S. *J. Phys. Chem. B* **2003**, *107*, 2837−2845.

(17) Genick, U. K.; Borgstahl, G. E.; Ng, K.; Ren, Z.; Pradervand, C.; Burke, P. M.; Srajer, V.; Teng, T. Y.; Schildkamp, W.; McRee, D. E.; Moffat, K.; Getzoff, E. D. *Science* **1997**, *275*, 1471−1475.

(18) Rubinstenn, G.; Vuister, G. W.; Mulder, F. A. A.; Dux, P. E.; Boelens, R.; Hellingwerf, K. J.; Kaptein, R. *Nat. Struct. Biol.* **1998**, *5*, 568−570.

(19) Hoff, W. D.; Xie, A.; Van Stokkum, I. H. M.; Tang, X.-j.; Gural, J.; Kroon, A. R.; Hellingwerf, K. J. *Biochemistry* **1999**, *38*, 1009−1017.

(20) Kandori, H.; Iwata, T.; Hendriks, J.; Maeda, A.; Hellingwerf, K. J. *Biochemistry* **2000**, *39*, 7902−7909.

(21) Brudler, R.; Rammelsberg, R.; Woo, T. T.; Getzoff, E. D.; Gerwert, K. *Nat. Struct. Biol.* **2001**, *8*, 265−270.

(22) Imamoto, Y.; Kamikubo, H.; Harigai, M.; Shimizu, N.; Kataoka, M. *Biochemistry* **2002**, *41*, 13595−13601.

(23) Hendriks, J.; Gensch, T.; Hviid, L.; van der Horst, M. A.; Hellingwerf, K. J.; van Thor, J. J. *Biophys. J.* **2002**, *82*, 1632−1643.

(24) Gensch, T.; Hendriks, J.; Hellingwerf, K. J. *Photochem. Photobiol. Sci.* **2004**, *3*, 531−536.

(25) Joshi, C. P.; Borucki, B.; Otto, H.; Meyer, T. E.; Cusanovich, M. A.; Heyn, M. P. *Biochemistry* **2005**, *44*, 656−665.

(26) Harigai, M.; Yasuda, S.; Imamoto, Y.; Yoshihara, F.; Tokunaga, F.; Kataoka, M. *J. Biochem.* **2001**, *130*, 51−56.

(27) Harigai, M.; Imamoto, Y.; Kamikubo, H.; Yamazaki, Y.; Kataoka, M. *Biochemistry* **2003**, *42*, 13893−13900.

(28) van der Horst, M. A.; van Stokkum, I. H.; Crielaard, W.; Hellingwerf, K. J. *FEBS Lett.* **2001**, *497*, 26−30.

(29) Borucki, B.; Devanathan, S.; Otto, H.; Cusanovich, M. A.; Tollin, G.; Heyn, M. P. *Biochemistry* **2002**, *41*, 10026−10037.

(30) Unno, M.; Kumauchi, M.; Hamada, N.; Tokunaga, F.; Yamauchi, S. *J. Biol. Chem.* **2004**, *279*, 23855−23858.

(31) Chosrowjan, H.; Taniguchi, S.; Mataga, N.; Unno, M.; Yamauchi, S.; Hamada, N.; Kumauchi, M.; Tokunaga, F. *J. Phys. Chem. B* **2004**, *108*, 2686−2698.

(32) Pan, D.; Philip, A.; Hoff, W. D.; Mathies, R. A. *Biophys. J.* **2004**, *86*, 2374−2382.

(33) Zhou, Y.; Ujj, L.; Meyer, T. E.; Cusanovich, M. A.; Atkkinson, G. H. *J. Phys. Chem. A* **2001**, *105*, 5719−5726.

(34) Imamoto, Y.; Mihara, K.; Hisatomi, O.; Kataoka, M.; Tokunaga, F.; Bojkova, N.; Yoshihara, K. *J. Biol. Chem.* **1997**, *272*, 12905−12908.

(35) Harada, I.; Takeuchi, H. In *Spectroscopy of Biological Systems*; Clark, R. J. H., Hester, R. E., Eds.; Advances in Spectroscopy 13; John Wiley & Sons: Chichester, UK, 1986; pp 113−175.

(36) Austin, J. C.; Jordan, T.; Spiro, T. G. In *Biomolecular Spectroscopy, Part A*; Clark, R. J. H., Hester, R. E., Eds.; Advances in Spectroscopy 20; John Wiley & Sons: Chichester, UK, 1993; pp 55−127.

(37) Unno, M.; Sano, R.; Masuda, S.; Ono, T.; Yamauchi, S. *J. Phys. Chem. B* **2005**, *109*, 12620−12626.

(38) Imamoto, Y.; Ito, T.; Kataoka, M.; Tokunaga, F. *FEBS Lett.* **1995**, *374*, 157−160.

(39) Mihara, K.; Hisatomi, O.; Imamoto, Y.; Kataoka, M.; Tokunaga, F. *J. Biochem.* **1997**, *121*, 876−880.

(40) Dudik, J. M.; Johnson, C. K.; Asher, S. A. *J. Chem. Phys.* **1985**, *82*, 1732−1740.

(41) Siamwiza, M. N.; Lord, R. C.; Chen, M. C.; Takamatsu, T.; Harada, I.; Matsuura, H.; Shimanouchi, T. *Biochemistry* **1975**, *14*, 4870−4876.

(42) Fodor, S. P. A.; Copeland, R. A.; Grygon, C. A.; Spiro, T. G. *J. Am. Chem. Soc.* **1989**, *111*, 5509−5518.

(43) Zhao, X.; Chen, R.; Tengroth, C.; Spiro, T. G. *Appl. Spectrosc.* **1999**, *53*, 1200−1205.

(44) Mathies, R. A.; Smith, S. O.; Palings, I. In *Biological Applications of Raman Spectroscopy*; Spiro, T. G., Ed.; Wiley-Interscience: New York, 1988; Vol. II, pp 59−108.

(45) Takeuchi, H.; Watanabe, N.; Harada, I. *Spectrochim. Acta, Part A* **1988**, *44A*, 749−761.

(46) Brudler, R.; Meyer, T. E.; Genick, U. K.; Devanathan, S.; Woo, T. T.; Millar, D. P.; Gerwert, K.; Cusanovich, M. A.; Tollin, G.; Getzoff, E. D. *Biochemistry* **2000**, *39*, 13478−13486.

(47) Meyer, T. E.; Devanathan, S.; Woo, T.; Getzoff, E. D.; Tollin, G.; Cusanovich, M. A. *Biochemistry* **2003**, *42*, 3319−3325.

(48) Derix, N. M.; Wechselberger, R. W.; van der Horst, M. A.; Hellingwerf, K. J.; Boelens, R.; Kaptein, R.; van Nuland, N. A. J. *Biochemistry* **2003**, *42*, 14501−14506.

(49) Miura, T.; Takeuchi, H.; Harada, I. *Biochemistry* **1988**, *27*, 88−94.

(50) Miura, T.; Takeuchi, H.; Harada, I. *J. Raman Spectrosc.* **1989**, *20*, 667−671.

(51) Rodgers, K. R.; Su, C.; Subramaniam, S.; Spiro, T. G. *J. Am. Chem. Soc.* **1992**, *114*, 3697−3709.

(52) Takeuchi, H.; Watanabe, N.; Satoh, U.; Harada, I. *J. Raman Spectrosc.* **1989**, *20*, 233−237.

(53) Schmidt, V.; Pahl, R.; Srajer, V.; Anderson, S.; Ren, Z.; Ihee, H.; Rajagopal, S.; Moffat, K. *Proc. Natl. Acad. Sci. U.S.A.* **2004**, *101*, 4799−4804.

(54) Matsuno, M.; Takeuchi, H. *Bull. Chem. Soc. Jpn.* **1998**, *71*, 851−857.

(55) Harada, I.; Miura, T.; Takeuchi, H. *Spectrochim. Acta, Part A* **1986**, *42A*, 307−312.

(56) Rodriguez-Mendieta, I. R.; Spence, G. R.; Gell, C.; Radford, S. E.; Smith, D. A. *Biochemistry* **2005**, *44*, 3306−3315.